mathematics

Article

Asian Option Pricing Under a Two-Factor Stochastic Volatility with a Stochastic Long-Term Mean

Junkee Jeon [1] and Geonwoo Kim [2,*]

[1] Department of Applied Mathematics, Kyung Hee University, Yongin 17104, Republic of Korea; junkeejeon@khu.ac.kr
[2] School of Natural Sciences, Seoul National University of Science and Technology, Seoul 01811, Republic of Korea
* Correspondence: geonwoo@seoultech.ac.kr; Tel.: +82-02-970-6271

Abstract

This paper studies the valuation of continuously monitored geometric Asian options under a two-factor stochastic volatility model with stochastic long-term variance levels. We derive the joint characteristic function required for continuous geometric averaging and obtain analytical pricing formulas for fixed-strike call and put options through Fourier inversion. The analytical formulas are verified by comparison with Monte Carlo simulation. Numerical experiments show that option values are particularly sensitive to the initial variance levels, while changes in the trends of the stochastic long-term means and leverage correlations also affect prices across strikes. The proposed approach extends double Heston Asian option pricing while maintaining computational tractability, and it provides a flexible method for examining the impact of time-varying long-term volatility expectations.

Keywords: asian option; stochastic volatility; stochastic long-term mean; characteristic function

MSC: 91G20; 91G40

1. Introduction

Asian options are path-dependent derivatives whose payoff is determined by an average of the underlying asset price over a specified monitoring period. Averaging reduces the influence of temporary price fluctuations and limits exposure to manipulation at a single fixing date. These features make Asian options useful for hedging commodity, foreign-exchange, and other accumulated price exposures. They are also generally less expensive than otherwise comparable plain-vanilla options. Their practical advantages come at the cost of a more difficult valuation problem because the payoff depends on the price history rather than only on the price observed at maturity. Among the principal contract types, geometric Asian options are especially important because they provide analytically tractable benchmarks and useful control variates for the numerical valuation of arithmetic Asian options [1].

The Black–Scholes framework provides a convenient starting point for option valuation, but its constant-volatility assumption is inconsistent with the volatility smiles, skews, clustering, and maturity effects observed in financial markets. The Heston model addresses this limitation by introducing a mean-reverting stochastic variance process while retaining analytical tractability [2]. This tractability has made the model a natural foundation for the valuation of path-dependent derivatives. Kim and Wee [3], for example, obtained explicit

Check for updates

Academic Editor: Anatoliy Swishchuk

Received: 18 August 2026
Revised: 6 September 2026
Accepted: 8 September 2026
Published: 18 September 2026

valuation formulas for geometric Asian options under Heston stochastic volatility. Their analysis demonstrates that transform approaches can successfully incorporate continuous averaging while maintaining analytical valuation.

A single variance factor may nevertheless be too restrictive when short- and long-horizon volatility risks behave differently. Christoffersen, Heston, and Jacobs [4] demonstrated that multifactor stochastic-volatility models provide a substantially richer description of the shape and term structure of the index-option smirk. The additional variance factor allows the model to distinguish persistent movements in the general volatility level from faster changes in the slope of the implied-volatility surface. This empirical motivation is particularly relevant for Asian options because averaging makes their values sensitive to volatility over the entire contract period rather than only near maturity.

The multifactor approach has already been applied to Asian option valuation. Zhong and Deng [5] combined two Heston variance factors with a stochastic interest rate and derived explicit pricing formulas for continuously monitored geometric Asian options. Their study established that a double-Heston structure can remain tractable even for path-dependent claims. However, the long-term mean of each variance factor is assumed to be constant. Consequently, the model allows current variance to fluctuate but does not permit the levels toward which the variance factors revert to change over time.

Recent studies have extended Asian option pricing in several other directions. Wang [6] examined defaultable Asian options under correlated time-varying variance and default intensity using GARCH models, which are frequently used in deep learning applications for time series forecasting [7–9]. Wang and Deng [10] considered geometric Asian extremum options in a model incorporating long-range dependence and jumps. Yin and Jia [11] obtained geometric and arithmetic Asian option prices in an uncertain mean-reverting market. More recently, Wang and Zhang [12] developed a framework for vulnerable geometric Asian options that incorporates multiple volatility factors, jumps, stochastic interest rates, and counterparty default. These studies demonstrate the continuing development of Asian option models and the importance of accounting for multiple sources of uncertainty. They do not, however, investigate the effect of time-varying long-term variance levels in a two-factor stochastic-volatility setting.

The assumption of a constant long-term variance level can be restrictive when the volatility term structure changes across market regimes. He and Chen [13] addressed this issue by allowing the long-term mean of Heston variance to evolve stochastically. Their model preserves analytical tractability and provides an analytical valuation formula for European options. Subsequent research has shown that this specification can be incorporated into more elaborate derivative pricing environments. Cho and Kim [14] combined stochastic long-term variance levels with multifactor volatility, counterparty credit risk, and stochastic liquidity. Jeon and Kim [15] likewise demonstrated that a multifactor state structure can remain analytically manageable when stochastic volatility and stochastic interest rates are considered together. These developments confirm the usefulness of stochastic long-term means, but the existing analytical results mainly concern European payoffs rather than continuously averaged prices.

This paper connects the multifactor Asian option literature with the stochastic long-term mean literature. We consider continuously monitored fixed-strike geometric Asian options under a two-factor stochastic volatility model in which each variance factor reverts toward its own stochastic long-term level. The two variance factors may have different adjustment speeds, leverage effects, volatilities, and long-term-mean dynamics. As a result, the model can distinguish between changes in current market volatility and changes in the longer-term volatility environment that market participants predict.

The closest benchmark to the present study is Zhong and Deng [5], who price continuously monitored geometric Asian options under a double-Heston model with a stochastic interest rate. Their two variance factors, however, revert to fixed long-term levels. Our analysis instead allows each factor to revert to its own stochastic long-term target and derives the joint transform required for continuous averaging in the resulting enlarged state space. Compared with He and Chen [13], who consider a one-factor stochastic-long-term-mean model for European options, the present framework introduces two volatility horizons and a path-dependent payoff. Recent Asian-option models have incorporated long-range dependence, jumps, multi-asset dynamics, stochastic interest rates, and counterparty default [10,16–18]. These extensions address different sources of risk but do not isolate how time-varying long-term variance targets propagate through a two-factor mean-reversion structure into a continuously averaged payoff. We therefore view the contribution as an analytically tractable integration of established ingredients.

The contributions of this paper are as follows. First, we formulate a tractable two-factor stochastic-volatility model with stochastic long-term variance levels for geometric Asian option valuation. The framework includes several important benchmark models as special cases, including the standard Heston model, the constant-mean double-Heston model, and the one-factor stochastic-long-term-mean model. Second, we derive the joint characteristic function needed for continuously monitored geometric averaging and use it to obtain explicit valuation formulas for fixed-strike call and put options. Third, we validate the analytical prices against Monte Carlo simulation and examine the effects of the initial asset price, trends in the stochastic long-term means, leverage correlations, initial variance levels, strike, and maturity. The numerical results demonstrate how changes in long-term volatility expectations are gradually reflected in Asian option prices through the mean-reversion mechanism and how their effects differ from changes in current variance.

The remainder of the paper is organized as follows. Section 2 introduces the risk-neutral model and defines the continuously monitored geometric average. Section 3 derives the joint characteristic function and the option pricing formulas. Section 4 presents the numerical analysis and Monte Carlo validation. Section 5 concludes the paper.

2. Model Formulation

Let $(\Omega, \mathcal{F}, (\mathcal{F}_t)_{t\geq 0}, \mathbb{Q})$ be a filtered probability space satisfying the usual conditions, where $\mathbb{Q}$ is the risk-neutral measure. We consider a two-factor stochastic volatility model. Then, the underlying asset under the measure $\mathbb{Q}$ is given by

$$\frac{\mathrm{d}S_t}{S_t} = r\,\mathrm{d}t + \sqrt{V_{1,t}}\,\mathrm{d}W_{1,t} + \sqrt{V_{2,t}}\,\mathrm{d}W_{2,t}, \tag{1}$$

where $r \geq 0$ is risk-free interest rate. Following He and Chen [13], for $j = 1, 2$, the variance factor and its stochastic long-term mean follow

$$\mathrm{d}V_{j,t} = \kappa_j(\Theta_{j,t} - V_{j,t})\,\mathrm{d}t + \sigma_j\sqrt{V_{j,t}}\,\mathrm{d}Z_{j,t}, \tag{2}$$

$$\mathrm{d}\Theta_{j,t} = \lambda_j\,\mathrm{d}t + \eta_j\,\mathrm{d}B_{j,t}. \tag{3}$$

For $j = 1, 2$, $W_{j,t}$, $Z_{j,t}$ and $B_{j,t}$ are the standard Brownian motions, and the instantaneous correlations are

$$\mathrm{d}\langle W_j, Z_j\rangle_t = \rho_j\,\mathrm{d}t, \qquad -1 < \rho_j < 1, \tag{4}$$

and all other Brownian motions are independent. In particular, each B_j is independent of all other Brownian motions.

https://doi.org/10.3390/math14183393

Remark 1 (Finite-horizon admissibility)**.** *Equation (3) implies*

$$\Theta_{j,t} = \Theta_{j,0} + \lambda_j t + \eta_j B_{j,t},$$

so that the stochastic long-term mean has Gaussian support and is not globally constrained to be nonnegative. Consequently, the model does not guarantee the non-negativity of $V_{j,t}$ for arbitrary parameter values and arbitrarily long horizons. We therefore interpret the specification as a finite-horizon affine approximation and restrict the numerical analysis to parameter sets for which the probability that $\Theta_{j,t}$ reaches zero over the option horizon is negligible. For $\eta_j > 0$ and $\Theta_{j,0} > 0$,

$$\mathbb{P}\left(\inf_{0\le s\le T}\Theta_{j,s} \le 0\right) = \Phi\left(\frac{-\Theta_{j,0} - \lambda_j T}{\eta_j\sqrt{T}}\right) + \exp\left(-\frac{2\lambda_j\Theta_{j,0}}{\eta_j^2}\right)\Phi\left(\frac{-\Theta_{j,0} + \lambda_j T}{\eta_j\sqrt{T}}\right).$$

Under the baseline parameters and $T = 2$, these probabilities are approximately 1.10×10^{-4} and 1.45×10^{-4} for Factors 1 and 2, respectively. When the long-term-mean path remains nonnegative, the square-root variance equation retains its usual nonnegative boundary behavior. Nevertheless, the Gaussian support of $\Theta_{j,t}$ is a limitation of the analytically tractable specification. A positivity-preserving stochastic long-term mean would lead to a different transform system and is left for future research.

Let $X_t = \log S_t$. Itô's formula gives

$$\mathrm{d}X_t = \left(r - \frac{1}{2}\sum_{j=1}^{2} V_{j,t}\right)\mathrm{d}t + \sum_{j=1}^{2}\sqrt{V_{j,t}}\,\mathrm{d}W_{j,t}. \tag{5}$$

For maturity $T > 0$, let us define

$$L_t = \frac{1}{T}\int_0^t X_s\,\mathrm{d}s, \qquad G_T = e^{L_T} = \exp\left(\frac{1}{T}\int_0^T \log S_s\,\mathrm{d}s\right). \tag{6}$$

Then, the fixed-strike call and put payoffs are $(G_T - K)^+$ and $(K - G_T)^+$, and their prices are given by

$$C_{\text{fix}} = e^{-rT}\mathbb{E}^{\mathbb{Q}}\left[(G_T - K)\mathbf{1}_{\{L_T > \log K\}}\right]$$
$$P_{\text{fix}} = e^{-rT}\mathbb{E}^{\mathbb{Q}}\left[(K - G_T)\mathbf{1}_{\{L_T \le \log K\}}\right],$$

where $\mathbf{1}_{\{.\}}$ is an indicator function.

3. Pricing of Asian Options

In this section, we study the pricing of Asian options under the proposed model. To price the options, we adopt the characteristic function approach. The joint characteristic function for the underlying asset is defined as

$$\Psi_t(u, w) = e^{-r(T-t)}\mathbb{E}^{\mathbb{Q}}\left[e^{\mathrm{i}uX_T + \mathrm{i}wL_T} \mid \mathcal{F}_t\right], \tag{7}$$

where $(u, w) \in \mathbb{C}^2$ and $0 \le t \le T$.

Theorem 1. *Let $\tau = T - t$ and*

$$b(\tau) = \mathrm{i}u + \mathrm{i}w\frac{\tau}{T}. \tag{8}$$

Then

$$\Psi_t(u,w) = \exp\left(A(\tau) + b(\tau)X_t + \mathrm{i}wL_t + \sum_{j=1}^{2}\{C_j(\tau)V_{j,t} + D_j(\tau)\Theta_{j,t}\}\right), \tag{9}$$

where $A(0) = C_j(0) = D_j(0) = 0$ and

$$C_j' = \frac{1}{2}b^2 - \frac{1}{2}b + (\rho_j\sigma_j b - \kappa_j)C_j + \frac{1}{2}\sigma_j^2 C_j^2, \tag{10}$$

$$D_j' = \kappa_j C_j, \tag{11}$$

$$A' = r(b-1) + \sum_{j=1}^{2}\left(\lambda_j D_j + \frac{1}{2}\eta_j^2 D_j^2\right). \tag{12}$$

All coefficient functions on the right-hand sides are evaluated at τ. The coefficients admit the following explicit representation. Set

$$p = \mathrm{i}u, \qquad q = \frac{\mathrm{i}w}{T}, \qquad b(s) = p + qs, \qquad a_j = \frac{1}{2}\sigma_j^2, \tag{13}$$

and define

$$\beta_{j0} = \rho_j\sigma_j p - \kappa_j, \qquad \beta_{j1} = \rho_j\sigma_j q, \tag{14}$$

$$\gamma_0 = \frac{1}{2}(p^2 - p), \qquad \gamma_1 = q\left(p - \frac{1}{2}\right), \qquad \gamma_2 = \frac{1}{2}q^2. \tag{15}$$

Further, put

$$\omega_{j0} = a_j\gamma_0 + \frac{1}{2}\beta_{j1} - \frac{1}{4}\beta_{j0}^2, \tag{16}$$

$$\omega_{j1} = a_j\gamma_1 - \frac{1}{2}\beta_{j0}\beta_{j1}, \tag{17}$$

$$\omega_{j2} = a_j\gamma_2 - \frac{1}{4}\beta_{j1}^2 = \frac{1}{4}\sigma_j^2(1-\rho_j^2)q^2. \tag{18}$$

Suppose that $q \neq 0$. Since $|\rho_j| < 1$, $\omega_{j2} \neq 0$. Define

$$h_j = \frac{\omega_{j1}}{2\omega_{j2}}, \qquad \delta_j = \omega_{j0} - \frac{\omega_{j1}^2}{4\omega_{j2}},$$

$$\alpha_j = (-4\omega_{j2})^{1/4}, \qquad \nu_j = \frac{\delta_j}{\alpha_j^2} - \frac{1}{2}, \qquad z_j(s) = \alpha_j(s + h_j). \tag{19}$$

Let ${}_1F_1$ denote Kummer's confluent hypergeometric function and set

$$F_j(s) = e^{-z_j(s)^2/4}{}_1F_1\left(-\frac{\nu_j}{2}; \frac{1}{2}; \frac{z_j(s)^2}{2}\right), \tag{20}$$

$$G_j(s) = z_j(s)e^{-z_j(s)^2/4}{}_1F_1\left(\frac{1-\nu_j}{2}; \frac{3}{2}; \frac{z_j(s)^2}{2}\right). \tag{21}$$

With primes denoting derivatives with respect to s, define

$$W_j = F_j(0)G_j'(0) - F_j'(0)G_j(0), \tag{22}$$

$$v_j(s) = \frac{G_j'(0) + \frac{1}{2}\beta_{j0}G_j(0)}{W_j}F_j(s) - \frac{F_j'(0) + \frac{1}{2}\beta_{j0}F_j(0)}{W_j}G_j(s), \tag{23}$$

$$y_j(s) = \exp\left(\frac{1}{2}\beta_{j0}s + \frac{1}{4}\beta_{j1}s^2\right)v_j(s). \tag{24}$$

If $q = 0$, the corresponding expression is

$$d_j = \sqrt{\beta_{j0}^2 - 4a_j\gamma_0}, \tag{25}$$

$$y_j(s) = e^{\beta_{j0}s/2}\left[\cosh\left(\frac{d_js}{2}\right) - \frac{\beta_{j0}}{d_j}\sinh\left(\frac{d_js}{2}\right)\right], \tag{26}$$

where the continuous limit is used when $d_j = 0$. In both cases choose the continuous logarithm

$$\ell_j(s) = \log y_j(s), \qquad \ell_j(0) = 0, \tag{27}$$

which is well defined. Then

$$C_j(s) = -\frac{2}{\sigma_j^2}\frac{y_j'(s)}{y_j(s)}, \tag{28}$$

$$D_j(s) = -\frac{2\kappa_j}{\sigma_j^2}\ell_j(s), \tag{29}$$

$$A(s) = r\left((p-1)s + \frac{1}{2}qs^2\right) - \sum_{j=1}^{2}\frac{2\lambda_j\kappa_j}{\sigma_j^2}\int_0^s \ell_j(a)\,\mathrm{d}a + \sum_{j=1}^{2}\frac{2\eta_j^2\kappa_j^2}{\sigma_j^4}\int_0^s \ell_j(a)^2\,\mathrm{d}a. \tag{30}$$

Consequently, (9) can be written explicitly as

$$\Psi_t(u,w) = \exp\Bigg\{\mathrm{i}wL_t + (p+q\tau)X_t + r\left((p-1)\tau + \frac{1}{2}q\tau^2\right) + \sum_{j=1}^{2}\Bigg[-\frac{2V_{j,t}}{\sigma_j^2}\frac{y_j'(\tau)}{y_j(\tau)} - \frac{2\kappa_j\Theta_{j,t}}{\sigma_j^2}\ell_j(\tau) - \frac{2\lambda_j\kappa_j}{\sigma_j^2}\int_0^\tau \ell_j(a)\,\mathrm{d}a + \frac{2\eta_j^2\kappa_j^2}{\sigma_j^4}\int_0^\tau \ell_j(a)^2\,\mathrm{d}a\Bigg]\Bigg\}. \tag{31}$$

Proof. Set

$$Y_t = (X_t, L_t, V_{1,t}, V_{2,t}, \Theta_{1,t}, \Theta_{2,t})$$

and write a candidate transform as $F(\tau, \boldsymbol{y})$, where $\boldsymbol{y} = (x, \ell, v_1, v_2, \theta_1, \theta_2)$. The generator of Y is $\mathcal{L} = \mathcal{L}_\mathrm{d} + \mathcal{L}_\mathrm{q}$, with

$$\mathcal{L}_\mathrm{d} = \left(r - \frac{1}{2}\sum_{j=1}^{2}v_j\right)\partial_x + \frac{x}{T}\partial_\ell + \sum_{j=1}^{2}\kappa_j(\theta_j - v_j)\partial_{v_j} + \sum_{j=1}^{2}\lambda_j\partial_{\theta_j},$$

$$\mathcal{L}_\mathrm{q} = \frac{1}{2}\sum_{j=1}^{2}v_j\partial_{xx} + \frac{1}{2}\sum_{j=1}^{2}\sigma_j^2 v_j\partial_{v_jv_j} + \frac{1}{2}\sum_{j=1}^{2}\eta_j^2\partial_{\theta_j\theta_j} + \sum_{j=1}^{2}\rho_j\sigma_j v_j\partial_{xv_j}.$$

No mixed derivative involving a target variable occurs because every B_j is independent of the return and variance drivers. In time to maturity, the Feynman–Kac equation is

$$\partial_\tau F = \mathcal{L}F - rF, \qquad F(0,x,\ell,\boldsymbol{v},\boldsymbol{\theta}) = e^{\mathrm{i}ux+\mathrm{i}w\ell}. \tag{32}$$

Consider

$$f = \exp\left(A + bx + \mathrm{i}w\ell + \sum_{j=1}^{2}(C_j v_j + D_j\theta_j)\right). \tag{33}$$

Dividing the required derivatives by f gives

$$\frac{f_\tau}{f} = A' + b'x + \sum_{j=1}^{2}(C_j'v_j + D_j'\theta_j), \qquad \frac{f_x}{f} = b, \qquad \frac{f_{xx}}{f} = b^2, \qquad \frac{f_\ell}{f} = \mathrm{i}w,$$
$$\frac{f_{v_j}}{f} = C_j, \qquad \frac{f_{v_jv_j}}{f} = C_j^2, \quad \frac{f_{\theta_j}}{f} = D_j, \quad \frac{f_{\theta_j\theta_j}}{f} = D_j^2, \quad \frac{f_{xv_j}}{f} = bC_j.$$

Substitution into (32) produces the identity

$$\begin{aligned}\frac{\mathcal{L}f - rf}{f} &= r(b-1) + \frac{\mathrm{i}w}{T}x + \sum_{j=1}^{2}\left(\lambda_j D_j + \frac{1}{2}\eta_j^2 D_j^2\right)\\ &\quad + \sum_{j=1}^{2} v_j\left[\frac{1}{2}b^2 - \frac{1}{2}b - \kappa_j C_j + \rho_j\sigma_j bC_j + \frac{1}{2}\sigma_j^2 C_j^2\right] + \sum_{j=1}^{2}\theta_j\kappa_j C_j.\end{aligned} \tag{34}$$

Equating the coefficients of the linearly independent functions $1, x, v_1, v_2, \theta_1, \theta_2$ in f_τ/f and (34) yields

$$b' = \frac{\mathrm{i}w}{T}$$

together with (10)–(12). The terminal condition in (32) gives $b(0) = \mathrm{i}u$ and $A(0) = C_j(0) = D_j(0) = 0$. Integrating the equation for b proves (8). The Riccati right-hand side is continuous in τ.

It remains to prove the explicit representation. With the notation in (13)–(15), set

$$C_j(s) = -\frac{1}{a_j}\frac{y_j'(s)}{y_j(s)}. \tag{35}$$

Since $C_j(0) = 0$, the normalization may be chosen as $y_j(0) = 1$ and $y_j'(0) = 0$. Differentiating (35) and substituting it into (10) cancels the quadratic term and gives the linear equation

$$y_j''(s) - (\beta_{j0} + \beta_{j1}s)y_j'(s) + a_j(\gamma_0 + \gamma_1 s + \gamma_2 s^2)y_j(s) = 0. \tag{36}$$

Thus, the apparent nonlinear obstruction is only a Riccati representation of a second-order linear equation.

Write

$$y_j(s) = \exp\left(\frac{1}{2}\beta_{j0}s + \frac{1}{4}\beta_{j1}s^2\right)v_j(s). \tag{37}$$

Direct differentiation of (37), followed by use of (36), yields

$$v_j''(s) + (\omega_{j0} + \omega_{j1}s + \omega_{j2}s^2)v_j(s) = 0, \tag{38}$$

where the coefficients are exactly (16)–(18). When $q \neq 0$, complete the square and use $z = z_j(s)$ from (19). Since $\alpha_j^4 = -4\omega_{j2}$, Equation (38) becomes

$$\frac{\mathrm{d}^2 v_j}{\mathrm{d}z^2} + \left(\nu_j + \frac{1}{2} - \frac{z^2}{4}\right) v_j = 0. \tag{39}$$

This is Weber's equation. Its even and odd Kummer solutions are precisely (20) and (21); hence their Wronskian is nonzero. The initial conditions for (37) are

$$v_j(0) = 1, \qquad v_j'(0) = -\frac{1}{2}\beta_{j0}.$$

Solving the resulting two-by-two linear system for the coefficients of F_j and G_j gives (23). This proves (24). When $q = 0$, Equation (36) has constant coefficients. Its solution with the same initial conditions is (26).

Equation (28) follows from (35). Integrating $D_j' = \kappa_j C_j$ and using the continuous logarithm with $\ell_j(0) = 0$ gives (29). Finally, substitution of $b = p + qs$ and (29) into (12) gives (30). Inserting (28)–(30) into (9) proves (31). □

Using Theorem 1, we can derive the explicit pricing formulae of Asian options in the proposed model. More specifically, by inverting the characteristic function of the logarithm of the average prices, we can obtain the price of Asian options.

Write $\Psi(u, w) = \Psi_0(u, w)$ and define

$$M_G = \Psi(0, -\mathrm{i}) = e^{-rT}\mathbb{E}^{\mathbb{Q}}[G_T], \qquad P_0 = e^{-rT}. \tag{40}$$

For a characteristic function φ with $\varphi(0) = 1$, let

$$\mathcal{I}(k; \varphi) = \frac{1}{2} + \frac{1}{\pi}\int_0^\infty \mathrm{Re}\left[\frac{e^{-\mathrm{i}zk}\varphi(z)}{\mathrm{i}z}\right] \mathrm{d}z. \tag{41}$$

Equation (41) is the Gil–Pelaez inversion formula [19]. Based on these notations, the fixed-strike Asian option prices are given in the following Theorem.

Theorem 2 (Fixed-strike Asian options)**.** *For $K > 0$ and $k = \log K$, define*

$$\varphi_1(z) = \frac{\Psi(0, z - \mathrm{i})}{\Psi(0, -\mathrm{i})}, \qquad \varphi_2(z) = \frac{\Psi(0, z)}{\Psi(0, 0)}, \qquad z \in \mathbb{R}, \tag{42}$$

and

$$\Pi_1 = \frac{1}{2} + \frac{1}{\pi}\int_0^\infty \mathrm{Re}\left[\frac{e^{-\mathrm{i}zk}\varphi_1(z)}{\mathrm{i}z}\right] \mathrm{d}z, \tag{43}$$

$$\Pi_2 = \frac{1}{2} + \frac{1}{\pi}\int_0^\infty \mathrm{Re}\left[\frac{e^{-\mathrm{i}zk}\varphi_2(z)}{\mathrm{i}z}\right] \mathrm{d}z. \tag{44}$$

Then the fixed-strike geometric Asian call and put prices are

$$C_{\text{fix}} = \Psi(0, -\mathrm{i})\Pi_1 - K\Psi(0, 0)\Pi_2, \tag{45}$$

$$P_{\text{fix}} = K\Psi(0, 0)(1 - \Pi_2) - \Psi(0, -\mathrm{i})(1 - \Pi_1), \tag{46}$$

and hence

$$C_{\text{fix}} - P_{\text{fix}} = \Psi(0, -\mathrm{i}) - K\Psi(0, 0). \tag{47}$$

Proof. Define measures on $\mathcal{F}_T$ by

$$\frac{d\mathbb{Q}^G}{d\mathbb{Q}} = \frac{e^{-rT}G_T}{\Psi(0,-\mathrm{i})}, \qquad \frac{d\mathbb{Q}^0}{d\mathbb{Q}} = \frac{e^{-rT}}{\Psi(0,0)}. \tag{48}$$

Theorem 1 gives $\Psi(0,-\mathrm{i}) = e^{-rT}\mathbb{E}[G_T] > 0$ and $\Psi(0,0) = e^{-rT}$. For real z,

$$\mathbb{E}^{\mathbb{Q}^G}[e^{\mathrm{i}zL_T}] = \frac{e^{-rT}}{\Psi(0,-\mathrm{i})}\mathbb{E}^{\mathbb{Q}}[e^{(1+\mathrm{i}z)L_T}] = \varphi_1(z), \tag{49}$$

$$\mathbb{E}^{\mathbb{Q}^0}[e^{\mathrm{i}zL_T}] = \frac{e^{-rT}}{\Psi(0,0)}\mathbb{E}^{\mathbb{Q}}[e^{\mathrm{i}zL_T}] = \varphi_2(z). \tag{50}$$

Thus, Equations (43) and (44) and Gil–Pelaez inversion give

$$\mathbb{Q}^G(L_T > k) = \Pi_1, \qquad \mathbb{Q}^0(L_T > k) = \Pi_2.$$

Since $\{G_T > K\} = \{L_T > k\}$,

$$\begin{aligned} C_{\text{fix}} &= e^{-rT}\mathbb{E}^{\mathbb{Q}}\Big[(G_T - K)\mathbf{1}_{\{L_T > k\}}\Big] \\ &= \Psi(0,-\mathrm{i})\mathbb{Q}^G(L_T > k) - K\Psi(0,0)\mathbb{Q}^0(L_T > k), \end{aligned}$$

which proves (45). Decomposition over the complementary event gives

$$\begin{aligned} P_{\text{fix}} &= e^{-rT}\mathbb{E}^{\mathbb{Q}}\Big[(K - G_T)\mathbf{1}_{\{L_T \le k\}}\Big] \\ &= K\Psi(0,0)(1-\Pi_2) - \Psi(0,-\mathrm{i})(1-\Pi_1), \end{aligned}$$

which proves (46). Subtraction gives (47). □

Theorem 2 requires only one-dimensional Fourier integration. All model dependence is contained in the explicit joint characteristic function of Theorem 1.

4. Numerical Examples

In this section, we present numerical experiments to illustrate the analytical pricing formula derived in the previous section and to conduct sensitivity analyses with respect to key model parameters. In addition, we validate the accuracy and computational efficiency of our proposed Fourier inversion method by comparing the analytical results with Monte Carlo (MC) simulations.

Unless specified otherwise, the baseline parameter values used throughout the numerical illustrations are summarized in Table 1. We consider a two-factor stochastic volatility model with stochastic long-term mean levels, where Factor 1 represents a fast-reverting, highly volatile component ($\kappa_1 = 3.00, \sigma_1 = 0.35, \rho_1 = -0.70$), and Factor 2 captures a slow-reverting, persistent variance component ($\kappa_2 = 0.60, \sigma_2 = 0.18, \rho_2 = -0.25$). The initial asset price is set to $S_0 = 100$, and the risk-free interest rate is $r = 0.03$.

Table 1. Baseline parameters.

j	S_0	r	$V_{j,0}$	$\Theta_{j,0}$	κ_j	σ_j	ρ_j	λ_j	η_j
1	100	0.03	0.030	0.040	3.00	0.35	−0.70	0.002	0.008
2			0.020	0.025	0.60	0.18	−0.25	0.001	0.005

Figure 1 shows the fixed-strike geometric Asian call price as a function of the strike K for three maturities, $T = 0.5, 1$, and 2. As expected, the price is decreasing and convex in K

for every maturity, and increasing in T for each fixed strike, reflecting the added time value of the additional averaging period. The maturity effect is markedly stronger for larger strikes than for smaller ones: at $K = 110$ the price rises roughly six-fold between $T = 0.5$ and $T = 2$ (from 0.7198 to 4.3357; Table 2), whereas at $K = 90$ it increases by only about 30% (from 11.0258 to 14.3479), since deep in-the-money options are already close to their intrinsic value and are comparatively insensitive to the extra volatility accumulated over a longer averaging horizon.

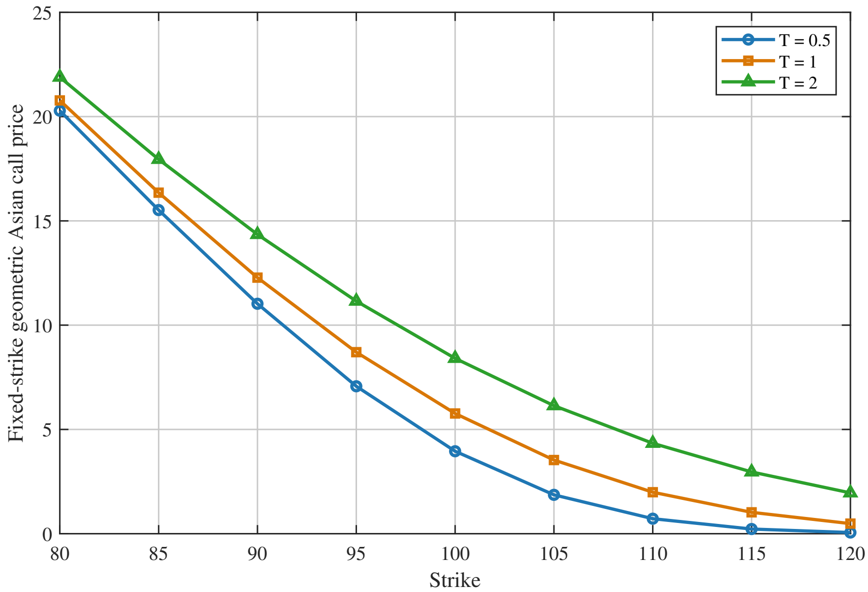

Figure 1. Fixed-strike geometric Asian call prices across strikes and maturities.

Figure 2 illustrates the effect of the initial asset price $S_0 \in \{90, 100, 110\}$ on the fixed-strike call price, with all other parameters held at baseline. The price is monotonically increasing in S_0 at every strike, and the three curves are close to vertical translates of one another, consistent with the approximate log-linear dependence of the geometric average G_T on S_0. The sensitivity to S_0 is largest for low strikes, where the option is deep in-the-money and its delta is close to one, and it narrows as the strike increases and the options move out-of-the-money.

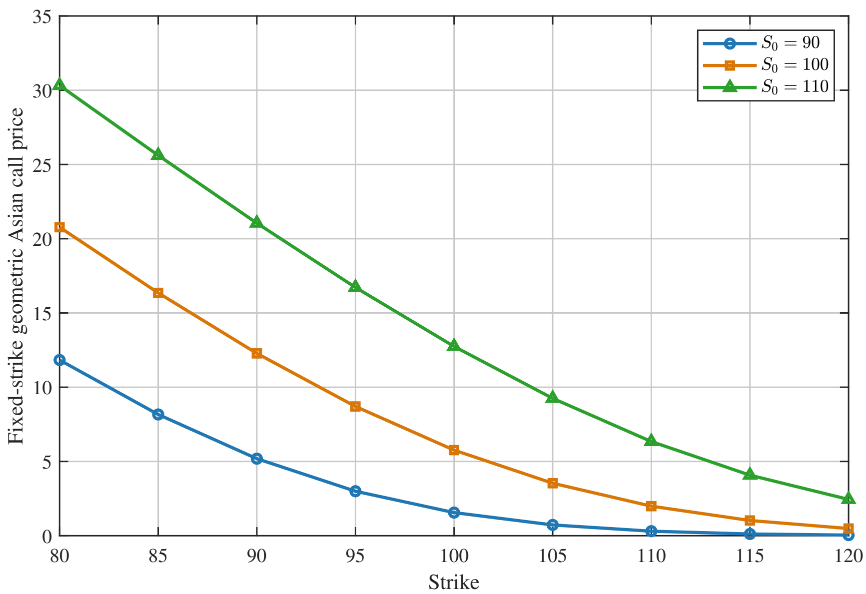

Figure 2. Fixed-strike geometric Asian call prices across strikes and initial underlying asset prices.

Figure 3 examines the factor-specific effects of the drift parameters of the stochastic long-term variance levels. In Figure 3a, λ_1 is varied, while λ_2 is fixed at its baseline value; on the other hand, Figure 3b varies λ_2 while keeping λ_1 fixed. In both cases, a larger drift parameter increases the option price because it raises the expected future level of the corresponding long-term variance target. Through the mean-reversion mechanism in the variance process, this higher target is gradually transmitted to the current variance and increases the variance accumulated over the averaging period. The resulting price effect is more visible for higher strikes, where option value depends more strongly on future volatility, while the curves remain relatively close for low strikes.

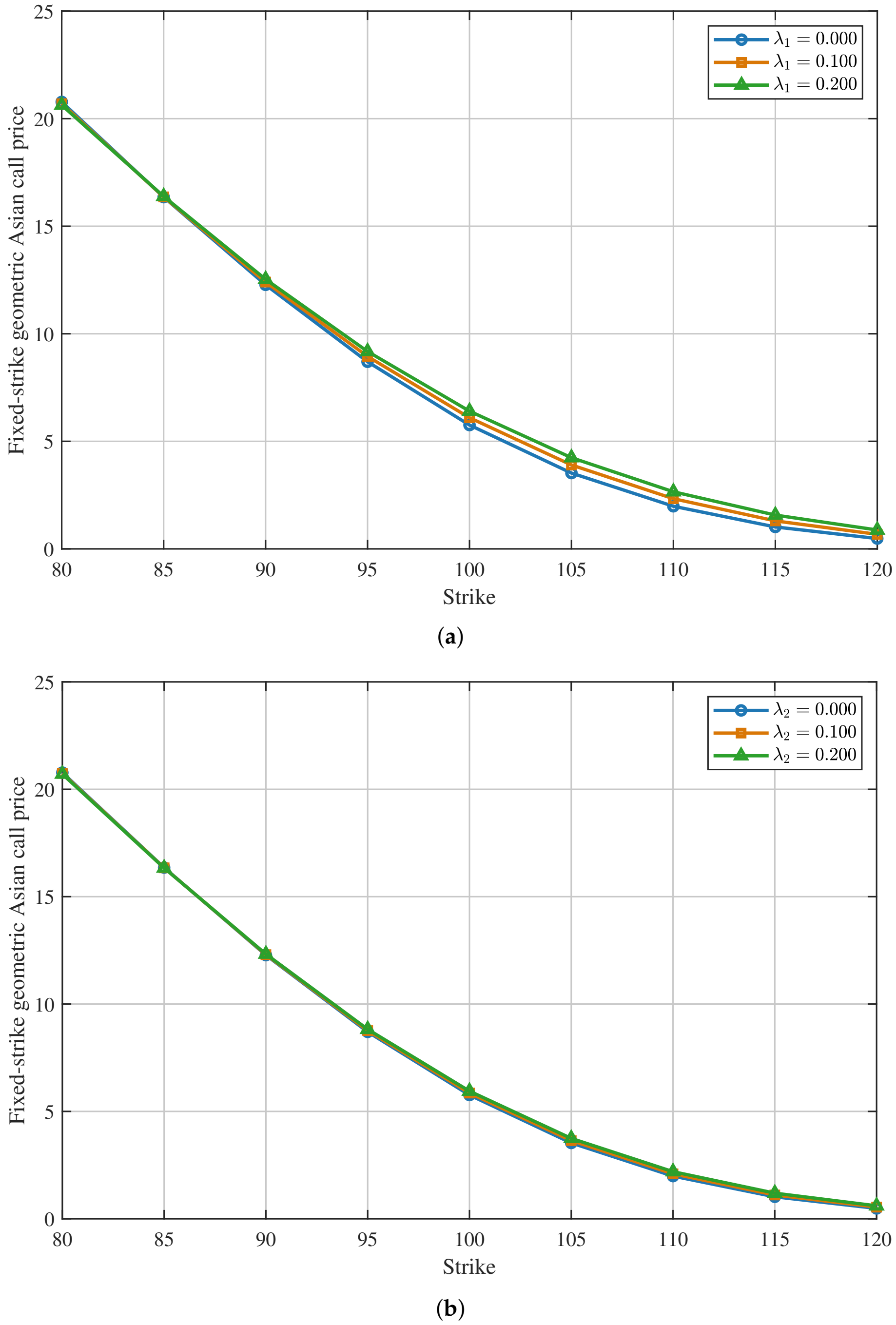

Figure 3. Fixed-strike geometric Asian call prices across strikes and long-term-mean drift parameters. (**a**) Sensitivity to λ_1 with λ_2 fixed at its baseline value. (**b**) Sensitivity to λ_2 with λ_1 fixed at its baseline value.

https://doi.org/10.3390/math14183393

The comparison of the two panels also reveals an important difference between the two variance factors. The effect of λ_1 is noticeably stronger than that of λ_2. This is consistent with the different mean-reversion speeds of the two factors. Since Factor 1 is fast reverting ($\kappa_1 = 3.00$), changes in its long-term target are transmitted relatively quickly to $V_{1,t}$. By contrast, Factor 2 is much more persistent ($\kappa_2 = 0.60$), so changes in its long-term target affect $V_{2,t}$ more gradually over the option horizon. Thus, the two long-term-mean drift parameters play economically distinct roles even though they enter the model through the same stochastic-target specification. The parameter values used in this sensitivity exercise are intended to illustrate these factor-specific effects rather than to represent a calibrated range.

Figure 4 investigates the factor-specific effects of the leverage correlations. Figure 4a varies ρ_1 over the range $\{-0.90, 0, 0.90\}$, while ρ_2 is fixed at its baseline value, and Figure 4b performs the corresponding experiment for ρ_2 while holding ρ_1 fixed. Unlike the long-term-mean drift parameters, the leverage correlations do not generate an approximately parallel shift in the option price curve. Instead, they mainly change its shape across strikes.

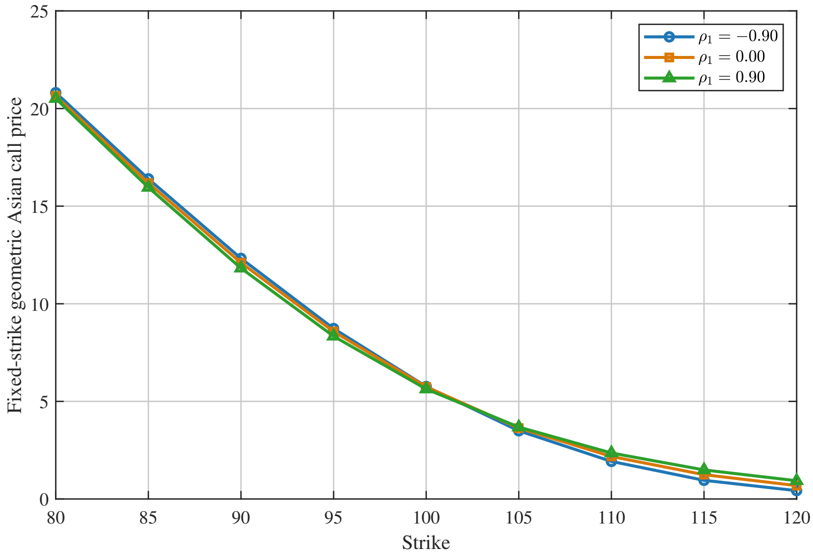

(**a**)

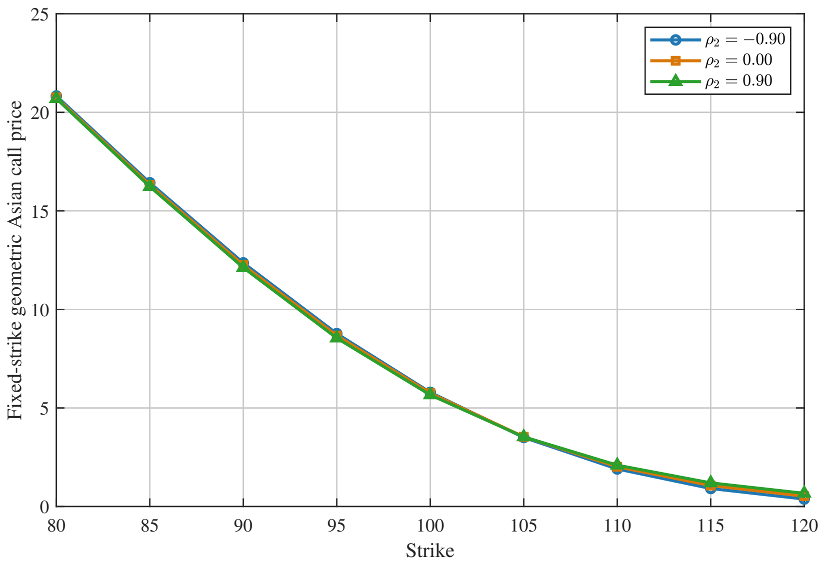

(**b**)

Figure 4. Fixed-strike geometric Asian call prices across strikes and leverage correlations. (**a**) Sensitivity to ρ_1 with ρ_2 fixed at its baseline value. (**b**) Sensitivity to ρ_2 with ρ_1 fixed at its baseline value.

In Figure 4a, the price curves are very close around the at-the-money region but separate more clearly toward the tails. A larger ρ_1 slightly lowers the prices of low-strike calls and raises the prices of high-strike calls. This pattern reflects the role of the return–variance correlation in shaping the skewness of the distribution of the underlying asset and, consequently, the distribution of its geometric average. A more negative leverage correlation places relatively more weight on adverse return–volatility comovements, whereas a more positive correlation shifts the relative tail behavior in the opposite direction. The effect therefore appears primarily as a change in the strike profile rather than as a uniform change in the overall price level.

Figure 4b shows the same qualitative mechanism for ρ_2, but the price differences are considerably smaller. This weaker sensitivity is consistent with the parameterization of the second variance factor: Factor 2 has a lower volatility-of-variance coefficient and evolves more persistently than Factor 1. Consequently, changing its instantaneous return–variance correlation has a more limited effect on the distribution of the continuously averaged price over the horizon considered. Taken together, Figure 4a,b show that the leverage effect is mainly transmitted through the first, faster volatility factor, while the second factor plays a more gradual role in shaping the volatility environment.

Figure 5 varies the common initial variance level while holding all other parameters at their baseline values. The option price increases monotonically with initial variance at every strike. Within the parameter ranges considered, changes in initial variance produce larger price shifts than changes in the long-term-mean drifts or leverage correlations. Economically, current variance immediately affects the uncertainty accumulated over the averaging period, whereas changes in the long-term mean are transmitted gradually through mean reversion. The leverage correlations mainly affect the shape of the price curve across strikes rather than generating a uniform change in its level.

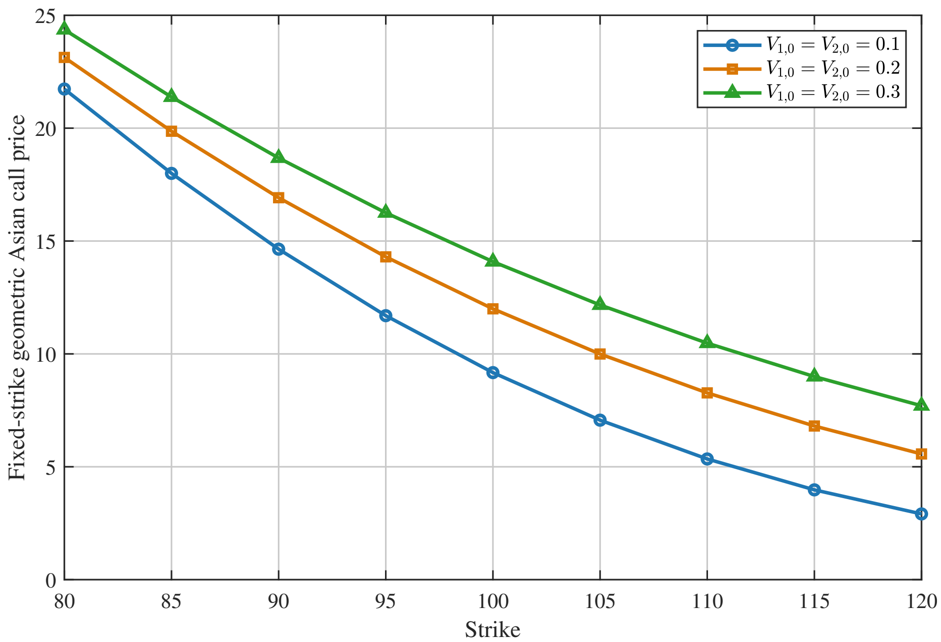

Figure 5. Fixed-strike geometric Asian call prices across strikes and initial volatility values.

For independent validation, we simulate 60,000 paths with 500 time steps per year. The stochastic long-term mean processes are simulated exactly at each time step, while the variance factors are approximated using the full-truncation Euler scheme [20]. The running log average is calculated using the trapezoidal rule.

Table 2 compares the Fourier-based prices C_{tr} obtained from Theorem 2 with the Monte Carlo estimates C_{MC} for nine combinations of maturity and strike. All Fourier-based prices lie within the corresponding 95% Monte Carlo confidence intervals, and the maximum absolute relative difference is approximately 0.52%. In addition, the Fourier prices are stable to six decimal places with 64 quadrature nodes. For a one-year maturity, the Monte Carlo method requires 30 million path-time-step updates, whereas the Fourier method involves only one-dimensional numerical integration and does not suffer from sampling error. These results confirm the accuracy and computational efficiency of the proposed pricing formula.

Table 2. Prices and Monte Carlo validation.

T	K	Price	Monte Carlo	95% Interval	Rel. Diff. (%)
0.5	90	11.0258	11.0013	$[10.9361, 11.0665]$	0.223
0.5	100	3.9543	3.9500	$[3.9061, 3.9939]$	0.110
0.5	110	0.7198	0.7207	$[0.7022, 0.7392]$	-0.127
1.0	90	12.2784	12.2591	$[12.1724, 12.3458]$	0.158
1.0	100	5.7646	5.7346	$[5.6704, 5.7987]$	0.523
1.0	110	1.9890	1.9828	$[1.9446, 2.0210]$	0.311
2.0	90	14.3479	14.3581	$[14.2398, 14.4764]$	-0.071
2.0	100	8.4077	8.4117	$[8.3162, 8.5072]$	-0.048
2.0	110	4.3357	4.3402	$[4.2699, 4.4105]$	-0.104

Table 3 separates the effects of the stochastic long-term means and the second variance factor. Under the baseline parameters, eliminating the diffusion terms of the long-term means has only a small effect on prices. However, the difference between the full model and the constant-target model increases with maturity and is more visible for out-of-the-money options. At $K = 110$, this difference increases from approximately 0.21% at $T = 0.5$ to 0.75% at $T = 2$, showing that changes in long-term volatility expectations are transmitted gradually over the averaging period.

Table 3. Comparison with nested benchmark models.

T	K	Full Model	$\eta_1 = \eta_2 = 0$	$\lambda_j = \eta_j = 0$	One-Factor SLM	Heston
0.5	90	11.0258	11.0258	11.0254	10.8176	10.8174
0.5	100	3.9543	3.9544	3.9525	3.2078	3.2056
0.5	110	0.7198	0.7198	0.7183	0.2178	0.2165
1.0	90	12.2784	12.2784	12.2757	11.8442	11.8420
1.0	100	5.7646	5.7649	5.7568	4.7693	4.7604
1.0	110	1.9890	1.9892	1.9808	1.0050	0.9959
2.0	90	14.3479	14.3484	14.3367	13.6254	13.6144
2.0	100	8.4077	8.4096	8.3815	7.1293	7.0998
2.0	110	4.3357	4.3379	4.3035	2.8791	2.8424

The second variance factor has a considerably larger effect. At $T = 2$ and $K = 110$, the full-model price is 4.3357, compared with 2.8791 under the one-factor stochastic-long-term-mean model and 2.8424 under the Heston model. Thus, the full-model price is approximately 52.5% higher than the Heston price in this case. Under the parameter setting considered, omitting the second volatility horizon can therefore produce materially lower prices for longer-maturity out-of-the-money Asian options. This finding is relevant to the pricing and risk management of contracts exposed to both short-term volatility shocks and persistent changes in the volatility environment.

5. Concluding Remarks

This paper developed a tractable framework for continuously monitored fixed-strike geometric Asian options under two-factor stochastic volatility with stochastic long-term variance levels. By allowing the long-term target of each variance factor to evolve over time, the model captures both current volatility conditions and changes in longer-term volatility expectations. Despite this richer structure and the path dependence of the payoff, we derived the required joint characteristic function and obtained analytical pricing formulas for call and put options through Fourier inversion. The resulting formulas are straightforward to implement and avoid computationally demanding multidimensional methods.

The analytical prices were reasonably close to Monte Carlo estimates across the tested strikes and maturities. The numerical results show that the initial variance levels have a pronounced effect on option values, while trends in the stochastic long-term means and leverage correlations generate additional and economically meaningful price variation across strikes. The proposed model therefore provides analytical tractability, computational efficiency, and more flexibility in representing the volatility dynamics relevant to Asian option valuation.

Author Contributions: J.J. and G.K. designed the model; J.J. and G.K. contributed to the analysis of the mathematical model; J.J. proved the propositions in the paper; J.J. and G.K. wrote the paper. All authors have read and agreed to the published version of the manuscript.

Funding: This research was supported by Seoul National University of Science and Technology.

Data Availability Statement: No new data were created or analyzed in this study. Data sharing is not applicable to this article.

Conflicts of Interest: The authors declare no conflicts of interest.

References

1. Kemna, A.G.Z.; Vorst, A.C.F. A Pricing Method for Options Based on Average Asset Values. *J. Bank. Financ.* **1990**, *14*, 113–129. [CrossRef]
2. Heston, S.L. A Closed-Form Solution for Options with Stochastic Volatility with Applications to Bond and Currency Options. *Rev. Financ. Stud.* **1993**, *6*, 327–343. [CrossRef]
3. Kim, B.; Wee, I.S. Pricing of Geometric Asian Options under Heston's Stochastic Volatility Model. *Quant. Financ.* **2014**, *14*, 1795–1809. [CrossRef]
4. Christoffersen, P.; Heston, S.; Jacobs, K. The Shape and Term Structure of the Index Option Smirk: Why Multifactor Stochastic Volatility Models Work So Well. *Manag. Sci.* **2009**, *55*, 1914–1932. [CrossRef]
5. Zhong, Y.; Deng, G. Geometric Asian Options Pricing under the Double Heston Stochastic Volatility Model with Stochastic Interest Rate. *Complexity* **2019**, *2019*, 4316272. [CrossRef]
6. Wang, X. Valuation of Asian Options with Default Risk under GARCH Models. *Int. Rev. Econ. Financ.* **2020**, *70*, 27–40. [CrossRef]
7. Koo, E.; Kim, G. A hybrid prediction model integrating GARCH models with a distribution manipulation strategy based on LSTM networks for stock market volatility. *IEEE Access* **2022**, *10*, 34743–34754. [CrossRef]
8. Tian, B.; Yan, T.; Yin, H. Forecasting the Volatility of CSI 300 Index with a Hybrid Model of LSTM and Multiple GARCH Models. *Comput. Econ.* **2025**, *66*, 1969–1999. [CrossRef]
9. Petrosino, L.; Bacco, L.; Salvati, G.; Merone, M.; Papi, M. A GARCH-temporal fusion transformer model for the volatility prediction of exchange traded funds. *Neural Comput. Appl.* **2025**, *37*, 21435–21458. [CrossRef]
10. Wang, R.; Deng, G. Pricing Geometric Asian Extremum Options under Mixed Fractional Brownian Motion with Jumps. *Jpn. J. Ind. Appl. Math.* **2025**, *42*, 2233–2261. [CrossRef]
11. Yin, X.; Jia, Z. Asian Option Pricing Formulas for Uncertain Financial Markets Based on the Exponential Ornstein–Uhlenbeck Model. *Mathematics* **2026**, *14*, 1545. [CrossRef]
12. Wang, L.; Zhang, R. Semi-Closed-Form Pricing of Vulnerable Geometric Asian Options under a Three-Factor Stochastic Volatility Jump-Diffusion Model with Stochastic Interest Rates. *Mathematics* **2026**, *14*, 2673. [CrossRef]
13. He, X.J.; Chen, W. A Closed-Form Pricing Formula for European Options under a New Stochastic Volatility Model with a Stochastic Long-Term Mean. *Math. Financ. Econ.* **2021**, *15*, 381–396. [CrossRef]

14. Cho, S.Y.; Kim, G. Analytically Pricing Vulnerable Options under the Stochastic Volatility Model with Stochastic Long-Term Mean and Stochastic Liquidity. *Commun. Nonlinear Sci. Numer. Simul.* **2026**, *161*, 110130. [CrossRef]
15. Jeon, J.; Kim, G. Analytical Pricing Vulnerable Options with Stochastic Volatility in a Two-Factor Stochastic Interest Rate Model. *Mathematics* **2025**, *13*, 2515. [CrossRef]
16. Chen, B.; Deng, G. Analytic approximations for European-style Asian spread options. *Aims Math.* **2024**, *9*, 11696–11717. [CrossRef]
17. Liu, K.; Peng, J.; Xu, C. Pricing geometric Asian options with liquidity risk under a regime-switching mixed fractional Brownian motion with jumps model. *Math. Comput. Simul.* **2026**, *249*, 264–284. [CrossRef]
18. Deng, G.; Hong, Z. Valuing Vulnerable Geometric Asian Basket Options Under Stochastic Volatility Jump Diffusion Model. *Comput. Econ.* **2026**, *67*, 2361–2397. [CrossRef]
19. Gil-Pelaez, J. Note on the inversion theorem. *Biometrika* **1951**, *38*, 481–482. [CrossRef]
20. Lord, R.; Koekkoek, R.; van Dijk, D. A comparison of biased simulation schemes for stochastic volatility models. *Quant. Financ.* **2010**, *10*, 177–194. [CrossRef]